
This is an electronic reprint of the original article.
This reprint may differ from the original in pagination and typographic detail.

Author(s): Koblmuller, G. & Reurings, F. & Tuomisto, Filip & Speck, J. S.
Title: Influence of Ga/N ratio on morphology, vacancies, and electrical transport in GaN grown by molecular beam epitaxy at high temperature
Year: 2010
Version: Final published version

Please cite the original version:

Koblmuller, G. & Reurings, F. & Tuomisto, Filip & Speck, J. S.. 2010. Influence of Ga/N ratio on morphology, vacancies, and electrical transport in GaN grown by molecular beam epitaxy at high temperature. Applied Physics Letters. Volume 97, Issue 19. 191915/1-3. ISSN 0003-6951 (printed). DOI: 10.1063/1.3514236

Rights: © 2010 American Institute of Physics. This article may be downloaded for personal use only. Any other use requires prior permission of the authors and the American Institute of Physics. The following article appeared in Applied Physics Letters. Volume 97, Issue 19 and may be found at <http://scitation.aip.org/content/aip/journal/apl/97/19/10.1063/1.3514236>.

All material supplied via Aaltodoc is protected by copyright and other intellectual property rights, and duplication or sale of all or part of any of the repository collections is not permitted, except that material may be duplicated by you for your research use or educational purposes in electronic or print form. You must obtain permission for any other use. Electronic or print copies may not be offered, whether for sale or otherwise to anyone who is not an authorised user.

Influence of Ga/N ratio on morphology, vacancies, and electrical transport in GaN grown by molecular beam epitaxy at high temperature

G. Koblmüller, F. Reurings, F. Tuomisto, and J. S. Speck

Citation: [Applied Physics Letters](#) **97**, 191915 (2010); doi: 10.1063/1.3514236

View online: <http://dx.doi.org/10.1063/1.3514236>

View Table of Contents: <http://scitation.aip.org/content/aip/journal/apl/97/19?ver=pdfcov>

Published by the [AIP Publishing](#)

Articles you may be interested in

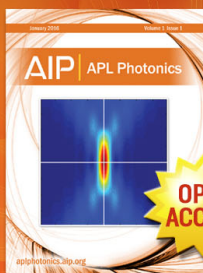
[Growth diagram of N-face GaN \(000 1⁻\) grown at high rate by plasma-assisted molecular beam epitaxy](#)
Appl. Phys. Lett. **104**, 012111 (2014); 10.1063/1.4861746

[Surface morphology evolution of m-plane \(1 1⁻ 00\) GaN during molecular beam epitaxy growth: Impact of Ga/N ratio, miscut direction, and growth temperature](#)
J. Appl. Phys. **114**, 023508 (2013); 10.1063/1.4813079

[Deep level transient spectroscopy in plasma-assisted molecular beam epitaxy grown Al 0.2 Ga 0.8 N / GaN interface and the rapid thermal annealing effect](#)
Appl. Phys. Lett. **97**, 112110 (2010); 10.1063/1.3491798

[High electron mobility GaN grown under N-rich conditions by plasma-assisted molecular beam epitaxy](#)
Appl. Phys. Lett. **91**, 221905 (2007); 10.1063/1.2817597

[Improved surface morphology in GaN homoepitaxy by NH₃-source molecular-beam epitaxy](#)
J. Vac. Sci. Technol. B **22**, 2158 (2004); 10.1116/1.1775202



Launching in 2016!
The future of applied photonics research is here

OPEN
ACCESS

AIP | APL
Photonics

Influence of Ga/N ratio on morphology, vacancies, and electrical transport in GaN grown by molecular beam epitaxy at high temperature

G. Koblmüller,^{1,3,a)} F. Reurings,² F. Tuomisto,² and J. S. Speck¹

¹Material Department, University of California, Santa Barbara, California 93106, USA

²Department of Applied Physics, Aalto University, 00076 Aalto, Finland

³Walter Schottky Institut and Physik Department, Technische Universität München, 85748 Garching, Germany

(Received 5 July 2010; accepted 20 October 2010; published online 12 November 2010)

The effect of Ga/N flux ratio on surface morphology, incorporation of point defects and electrical transport properties of GaN films grown by plasma-assisted molecular beam epitaxy in a recently developed high-temperature growth regime was investigated. The homoepitaxial (0001) GaN films grown at $\sim 780\text{--}790\text{ }^\circ\text{C}$ showed smoothest morphologies near the cross-over between N-rich and Ga-rich growth ($0.75 < \text{Ga}/\text{N} < 1.1$) contrasting previous observations for low-temperature growth. The higher-quality growth near $\text{Ga}/\text{N} \sim 1$ resulted from lower thermal decomposition rates and was corroborated by slightly lower Ga vacancy concentrations $[\text{V}_{\text{Ga}}]$, lower unintentional oxygen incorporation, and improved electron mobilities. The consistently low $[\text{V}_{\text{Ga}}]$, i.e., $\sim 10^{16}\text{ cm}^{-3}$ for all films attribute further to the significant benefits of the high-temperature growth regime. © 2010 American Institute of Physics. [doi:10.1063/1.3514236]

Progress in group-III nitride electronic devices has been largely aided by significant materials improvements using the versatile molecular beam epitaxy (MBE) growth technique.^{1–3} Plasma-assisted (PA)-MBE based on rf activated atomic nitrogen (N) has traditionally enabled high quality GaN growth at fairly low temperatures ($T \sim 650\text{--}740\text{ }^\circ\text{C}$) under kinetically limited group III-rich conditions.⁴ In low-T MBE-grown GaN, impurity incorporation, point defect densities, and electrical properties,⁵ were found extremely sensitive to growth stoichiometry (Ga/N flux ratio), i.e., both oxygen (O) and Ga vacancy (V_{Ga}) densities [mainly as V_{Ga} -donor impurity complexes, $\text{V}_{\text{Ga}}\text{-O}_\text{N}$ (Ref. 6)] were much higher in N-rich as in Ga-rich grown films.^{7–9} These $\text{V}_{\text{Ga}}\text{-O}_\text{N}$ complexes are acceptor states in unintentionally doped (UID) n-type GaN and cause electrical compensation.^{6,10–12}

Optimized films by Ga-rich/low-T PAMBE growth have, however, suffered from extreme growth control at the boundary for Ga droplet formation, and second, relatively large reverse-bias leakage currents through charged threading dislocations (TDs).¹³ Recently, we surpassed these problems by growth at much higher temperatures [i.e., region of thermal decomposition ($>760\text{ }^\circ\text{C}$)] and at surprisingly low Ga/N ratios ($\text{Ga}/\text{N} \leq 1$).^{14–16} The major benefits were much wider growth window for smooth GaN without excess metallic Ga nor additional defects, yielding the highest ever reported bulk room temperature (RT) electron mobilities ($>1150\text{ cm}^2/\text{V s}$).^{15,17} In addition, these conditions resulted in ultralow reverse bias leakage,¹⁸ in significant contrast to low-T grown GaN films. Despite these advances systematic studies of the effect of the Ga/N ratio on surface kinetics, native point defects, and electrical transport within this promising growth regime are still missing.

Resolving these critical properties was the aim of this letter, using atomic force microscopy (AFM), secondary ion mass spectroscopy (SIMS), positron annihilation spectroscopy (PAS) and Hall effect measurements for a set of high-T homoepitaxial (0001) GaN films.

The GaN films were grown in a Gen-II MBE system using effusion cells for Ga, and Si and a Veeco Unibulb radio frequency plasma source for active nitrogen. All high-T GaN films were $\sim 0.8\text{--}1\text{ }\mu\text{m}$ thick, lightly doped with Si (low- 10^{16} cm^{-3} region), and grown at constant $T \sim 780\text{--}790\text{ }^\circ\text{C}$ but variable Ga/N flux ratio. Details on source purity, flux, and growth temperature calibration as well as underlying buffer layer structure are reported elsewhere.¹⁵ The PAS experiments were performed at RT with a variable-energy positron beam and high purity Ge detectors.¹⁹

As substrates highly resistive (0001) GaN templates (Lumilog) with a TD density (TDD) of $\sim 5 \times 10^8\text{ cm}^{-2}$ were used. For the PAS investigations, we compared films grown on these GaN templates also with films on lower TDD GaN substrates, i.e., (i) on epitaxial lateral overgrowth (ELO) (0001) GaN with an average TDD $\sim 4 \times 10^7\text{ cm}^{-2}$ and (ii) on freestanding (0001) GaN with TDD $\sim 5 \times 10^6\text{ cm}^{-2}$.

Representative AFM morphologies for the high-T GaN films grown under different Ga/N ratios (range of 0.6–2.8) are shown in Fig. 1. The surfaces changed from terracelike structures (with multiple steps of c constant) under very Ga-rich conditions [Figs. 1(a) and 1(b)] to much smoother layer-by-layer-like morphologies under low Ga-rich and slightly N-rich growth [Figs. 1(c)–1(e)], and to increasingly pitted surfaces under more N-rich conditions [Fig. 1(f)]. Concurrently, the root-mean-square (rms) roughness over the selected $10 \times 10\text{ }\mu\text{m}^2$ area changed from 3.6 nm to 2.1, 0.8, 1.0, 1.2, and 3.8 nm consecutively from Figs. 1(a)–1(f).

While the layer-by-layer features in Figs. 1(c)–1(e) were similar to those found earlier for N-rich/high-T growth,¹⁵ the terracelike structure under more Ga-rich conditions was opposed to the hexagonal spiral hillocks common under Ga-rich/low-T conditions.⁵ The absence of spiral growth hillocks indicates an increased critical radius of curvature for two-dimensional (2D) island formation or spiral initiation, i.e., changes in step energy.^{4,5} Most striking, the tendency for the smoothest surfaces near the cross-over from N-rich to Ga-

rich growth was observed. The smoothest surfaces were found near the cross-over from N-rich to Ga-rich growth. The smoothest surfaces were found near the cross-over from N-rich to Ga-rich growth. The smoothest surfaces were found near the cross-over from N-rich to Ga-rich growth.

^{a)}Author to whom correspondence should be addressed. Electronic mail: gregor.koblmueller@wsi.tum.de.

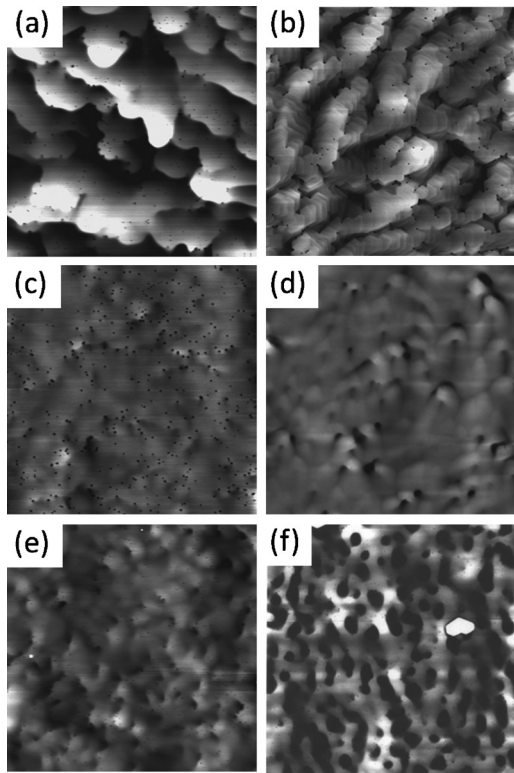


FIG. 1. $10 \times 10 \mu\text{m}^2$ AFM images of high-T PAMBE GaN films grown on standard (0001) GaN templates ($\text{TDD} \sim 5 \times 10^8 \text{ cm}^{-2}$) at fixed $T = 780^\circ\text{C}$ and N flux of 5 nm/min but variable Ga/N flux ratio of (a) 2.8, (b) 1.6, (c) 1.1, (d) 0.9, (e) 0.8, and (f) 0.6. The height scale is 10 nm.

rich growth ($\text{Ga}/\text{N} \sim 1$), is in complete difference to the required Ga-rich/near-Ga-droplet conditions ($\text{Ga}/\text{N} \gg 1$) for high-quality GaN at low-T ($< 750^\circ\text{C}$).⁴ We attribute this discrepancy to the modified surface growth kinetics under the influence of thermal decomposition at the high-T conditions,^{13,20} as discussed below. On the other hand, the more pitted surface for the very N-rich grown film [Fig. 1(f)] was associated with increased excess active N on the surface leading to larger surface diffusion barrier.^{4,21}

We note that light Si doping ($[\text{Si}] \sim 10^{16} \text{ cm}^{-3}$) had no influence on the surface kinetics, as confirmed by qualitatively similar morphology of undoped GaN films grown under identical conditions. Thus, the N-rich/ high-T growth did not result in antisurfactant behavior by Si, as found for highly Si-doped N-rich grown GaN films at lower T.²²

To identify the relation between Ga/N ratio, morphology and predominant point defects we used PAS to determine $[\text{V}_{\text{Ga}}]$ from typical positron-electron pair annihilation characteristics.¹⁹ The PAS measurements were conducted under different positron implantation energies in the 0–25 keV range while probing the positron trapping at Ga vacancies via Doppler broadening of the annihilation radiation line at 511 keV. The data were analyzed using the conventional S and W parameters, representing the fractions of annihilations with low and high momentum electrons.¹⁹

The S parameter measured as a function of positron implantation energy (mean implantation depth) is shown in Fig. 2 for selected high-T GaN films in reference to MBE grown p-type GaN, where positrons annihilate only in the GaN lattice.¹⁰ For low-energy positrons (0–10 keV) implanted near the sample surface ($\sim 0.25 \mu\text{m}$ thick surface region) the S parameters were not constant ($0.48 > S > 0.44$). With in-

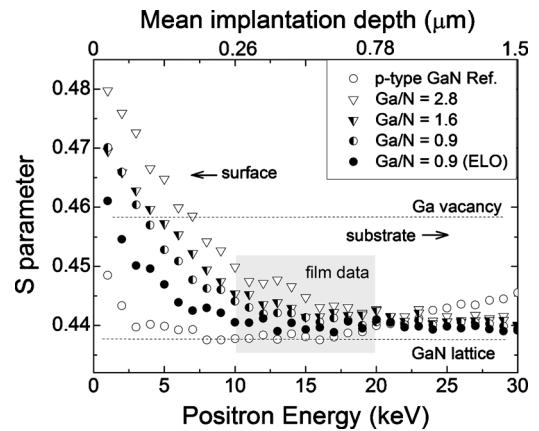


FIG. 2. S parameter measured as a function of positron implantation energy for high-T GaN films grown on both standard (0001) GaN templates ($\text{TDD} \sim 5 \times 10^8 \text{ cm}^{-2}$) and ELO-GaN template ($\text{TDD} \sim 4 \times 10^7 \text{ cm}^{-2}$) in reference to defect-free p-type GaN (as of Ref. 10).

creasing positron energy ($E > 10 \text{ keV}$) the positron diffusion to the surface decreased and the $S(E)$ curve saturated at constant levels of $S \sim 0.44$ – 0.45 , characteristic for the interior of the high-T GaN films.^{10,19} The S parameters were all higher than the respective value for the reference p-GaN sample, indicating that vacancy-type defects are present in the high-T GaN films. Analysis within the region of interest (sample depth of ~ 0.25 – $0.8 \mu\text{m}$) shows that these vacancy defects have a slightly higher density in the very Ga-rich grown films ($\text{Ga}/\text{N} \gg 1$) and reduced density with decreasing Ga/N ratio ($\text{Ga}/\text{N} \leq 1$). Moreover, the high-T GaN film grown on the ELO GaN template (TDD of $\sim 4 \times 10^7 \text{ cm}^{-2}$) exhibited S parameter very close to that for the perfect GaN lattice.

Further, the W parameter was determined and plotted against the S parameter (S - W plot not shown), evidencing the typical linearity of valence and core electron momentum distributions. This demonstrated that the positrons annihilated from two different states and were identified as delocalized state in the perfect GaN lattice and the localized state at the in-grown V_{Ga} ¹¹ allowing us to evaluate the absolute V_{Ga} density. By applying the positron trapping model,¹⁹ $[\text{V}_{\text{Ga}}]$ in the GaN films varied thus from ~ 2 – $6 \times 10^{16} \text{ cm}^{-3}$, with the lowest $[\text{V}_{\text{Ga}}]$ near or slightly below $\text{Ga}/\text{N} \sim 1$ [Fig. 3(a)]. Growth on lower-TDD GaN substrates at fixed Ga/N ratio of ~ 0.9 (N-rich growth) yielded slightly lower $[\text{V}_{\text{Ga}}]$ close to the detection limit of $\sim 1 \times 10^{16} \text{ cm}^{-3}$. Considering the significant change in TDD, this decrease in $[\text{V}_{\text{Ga}}]$ is negligible, indicating that V_{Ga} does not depend much on the presence of dislocations.²³ Overall, the values for $[\text{V}_{\text{Ga}}]$ reported here are very low, similar to the typical $[\text{V}_{\text{Ga}}]$ observed in highest-quality hydride vapor phase epitaxy GaN (Ref. 10) or Ga-rich/low-T-grown MBE-GaN (Ref. 7).

Analyzing the influence of Ga/N ratio on electrical transport, the RT Hall mobilities μ_e and respective bulk electron concentrations n_{bulk} for selected high-T GaN films are shown in Fig. 3(b). Consistent with the higher-quality morphology and lower $[\text{V}_{\text{Ga}}]$, the highest μ_e (i.e., > 870 and $> 1125 \text{ cm}^2/\text{V s}$) were achieved under slightly N-rich conditions for growth on standard and ELO-GaN templates respectively. Decreased μ_e at the more N-rich ($\text{Ga}/\text{N} \ll 1$) and Ga-rich ($\text{Ga}/\text{N} \gg 1$) sides was accompanied by slightly increased n_{bulk} from low- 10^{16} to $1 \times 10^{17} \text{ cm}^{-3}$. Since negatively charged V_{Ga} usually provide an acceptor in GaN, the

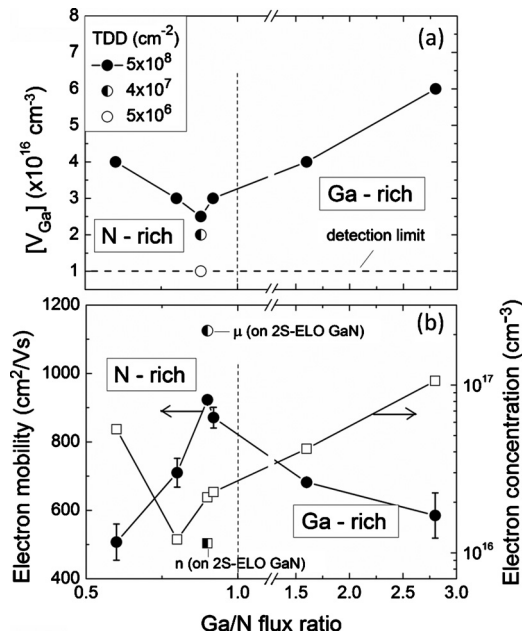


FIG. 3. (a) Calculated Ga vacancy concentration $[V_{Ga}]$ as function of Ga/N ratio for the high-T GaN films grown at fixed $T=780^\circ\text{C}$ and for different TDD-GaN substrates; (b) RT electron mobility and n-type carrier concentration for the same films as measured by Hall effect in vdP geometry.

increase in n_{bulk} must therefore arise from impurities such as (O) or (Si), which are predominant sources for n-type conductivity in GaN.²⁴ Based on SIMS measurements, the doped high-T GaN region showed only small variation in $[\text{Si}]$, i.e., $2 \times 10^{16} - 6 \times 10^{16} \text{ cm}^{-3}$, consistent with nominally supplied Si doping. On the other hand, UID $[\text{O}]$ was in the low- 10^{16} cm^{-3} region for GaN films grown at $\text{Ga}/\text{N} \sim 1$, and increased more toward $\sim 10^{17} \text{ cm}^{-3}$ when deviating from flux stoichiometry. Apart from the typical inaccuracy of SIMS these O-related doping effects are marginal but could be responsible for the slight increase in n_{bulk} , and correlate with the increase of $[V_{Ga}]$, since O forms high-binding energy complexes with V_{Ga} (Refs. 6 and 24) (evident in Fig. 3(a) and in agreement with previous PAS studies¹⁰⁻¹²).

Interpreting the relationship between morphology, $[V_{Ga}]$ and electrical properties, we considered the influence of Ga/N ratio on TD defects). Under variable Ga/N ratio, however, neither the TDD nor the relative proportion of TD-type (screw- versus mixed-, or edge-type component) was changed in the GaN films.¹⁸ This supports the notion that $[V_{Ga}]$ is completely independent of TDD,²³ and that the TDs do not contain vacancy defects in their core.²⁵

Thus, the trends for variable $[V_{Ga}]$ and $[\text{O}]$ most likely relate to differences in growth kinetics and associated surface morphology, through the competition between the forward (growth) and reverse (decomposition) reactions at high-T. Previous work demonstrated increased thermal decomposition rates for $\text{Ga}/\text{N} > 1$ as opposed to $\text{Ga}/\text{N} \leq 1$.²⁰ This explains the increased rms roughness under Ga-rich conditions, since with higher Ga desorption rates the Ga surface reactivity is reduced. Assuming that decomposition occurs by vacancy formation,²⁶ this suggests further a higher rate for vacancy generation under Ga-rich conditions.

Besides, decomposition also occurs near structural imperfections (dislocations, kinks, or step edges)²⁶ and is furthermore responsible for autodoping of donors in GaN.²⁷

This may also explain the higher propensity for step-edge

formation, more distinct open volume surface pits (i.e., at the termination of TDs), and slightly higher $[\text{O}]$ and n_{bulk} , which were observed more clearly in Ga-rich/high-T GaN films. In contrast, with more suppressed decomposition, N-rich/high-T grown GaN films resulted in smoother layer-by-layer like surfaces and decreased $[V_{Ga}]$. This interesting finding is in contrast to the common notion of much larger $[V_{Ga}]$ in N-rich/low-T GaN,^{23,27} and can be attributed to the much higher-quality growth under high-T growth conditions.

We gratefully acknowledge Evans Analytical group for SIMS measurements and B. Changala for assistance with AFM and Hall effect measurements. The work at UCSB was supported by AFOSR (Kitt Reinhardt, program manager) and ONR (Paul Maki, program manager). The work at Aalto University was partially funded by the MIDE program and the Academy of Finland. The work at UCSB made use of Central Facilities supported by the NSF MRSEC.

¹M. J. Manfra, N. G. Weimann, J. W. P. Hsu, L. N. Pfeiffer, K. W. West, and S. N. G. Chu, *Appl. Phys. Lett.* **81**, 1456 (2002).

²S. Rajan, P. Waltereit, C. Poblenz, S. J. Heikman, D. S. Green, J. S. Speck, and U. K. Mishra, *IEEE Electron Device Lett.* **25**, 247 (2004).

³C. Poblenz, A. L. Corrión, F. Recht, C. S. Suh, R. Chu, L. Shen, J. S. Speck, and U. K. Mishra, *IEEE Electron Device Lett.* **28**, 945 (2007).

⁴B. Heying, R. Averbeck, L. F. Chen, E. Haus, H. Riechert, and J. S. Speck, *J. Appl. Phys.* **88**, 1855 (2000).

⁵B. Heying, I. Smorchkova, C. Poblenz, C. Elsass, P. Fini, S. DenBaars, U. Mishra, and J. S. Speck, *Appl. Phys. Lett.* **77**, 2885 (2000).

⁶J. Neugebauer and C. G. Van de Walle, *Appl. Phys. Lett.* **69**, 503 (1996).

⁷C. R. Elsass, T. Mates, B. Heying, C. Poblenz, P. Fini, P. M. Petroff, S. P. Den Baars, and J. S. Speck, *Appl. Phys. Lett.* **77**, 3167 (2000).

⁸A. Hierro, A. R. Arehart, B. Heying, M. Hansen, U. K. Mishra, S. P. Den Baars, J. S. Speck, and S. A. Ringel, *Appl. Phys. Lett.* **80**, 805 (2002).

⁹M. Rummukainen, J. Oila, A. Laasko, K. Saarinen, A. J. Ptak, and T. H. Myers, *Appl. Phys. Lett.* **84**, 4887 (2004).

¹⁰J. Oila, J. Kivioja, V. Ranki, K. Saarinen, D. C. Look, R. J. Molnar, S. S. Park, S. K. Lee, and J. Y. Han, *Appl. Phys. Lett.* **82**, 3433 (2003).

¹¹S. Hautakangas, I. Makkonen, V. Ranki, M. J. Puska, K. Saarinen, X. Xu, and D. C. Look, *Phys. Rev. B* **73**, 193301 (2006).

¹²F. Tuomisto, K. Saarinen, T. Paskova, B. Monemar, M. Bockowski, and T. Suski, *J. Appl. Phys.* **99**, 066105 (2006).

¹³J. W. P. Hsu, M. J. Manfra, S. N. G. Chu, C. H. Chen, L. N. Pfeiffer, and R. J. Molnar, *Appl. Phys. Lett.* **78**, 3980 (2001).

¹⁴G. Koblmüller, S. Fernandez-Garrido, E. Calleja, and J. S. Speck, *Appl. Phys. Lett.* **91**, 161904 (2007).

¹⁵G. Koblmüller, F. Wu, T. Mates, J. S. Speck, S. Fernandez-Garrido, and E. Calleja, *Appl. Phys. Lett.* **91**, 221905 (2007).

¹⁶G. Koblmüller, R. Chu, F. Wu, U. K. Mishra, and J. S. Speck, *Appl. Phys. Express* **1**, 061103 (2008).

¹⁷G. Koblmüller, R. M. Chu, A. Raman, U. K. Mishra, and J. S. Speck, *J. Appl. Phys.* **107**, 043527 (2010).

¹⁸J. J. M. Law, E. T. Yu, G. Koblmüller, F. Wu, and J. S. Speck, *Appl. Phys. Lett.* **96**, 102111 (2010).

¹⁹K. Saarinen, P. Hautojärvi, and C. Corbel, in *Identification of Defects in Semiconductors*, Semiconductors and Semimetals Vol. 51A, edited by M. Stavola (Academic, New York, 1998), p. 209.

²⁰S. Fernández-Garrido, G. Koblmüller, E. Calleja, and J. S. Speck, *J. Appl. Phys.* **104**, 033541 (2008).

²¹T. Zywiets, J. Neugebauer, and M. Scheffler, *Appl. Phys. Lett.* **73**, 487 (1998).

²²A. L. Rosa and J. Neugebauer, *Phys. Rev. B* **73**, 205314 (2006).

²³J. Oila, V. Ranki, J. Kivioja, K. Saarinen, P. Hautojärvi, J. Likonen, J. M. Baranowski, K. Pakula, T. Suski, M. Leszczynski, and I. Grzegory, *Phys. Rev. B* **63**, 045205 (2001).

²⁴C. G. Van de Walle and J. Neugebauer, *J. Appl. Phys.* **95**, 3851 (2004).

²⁵J. Oila, K. Saarinen, A. E. Wickenden, D. D. Koleske, R. L. Henry, and M. E. Twigg, *Appl. Phys. Lett.* **82**, 1021 (2003).

²⁶N. Grandjean, J. Massies, F. Semond, S. Yu. Karpov, and R. A. Talalaev, *Appl. Phys. Lett.* **74**, 1854 (1999).

²⁷N. Newman, J. Ross, and M. Rubin, *Appl. Phys. Lett.* **62**, 1242 (1993).